

Symmetric Control Design for Multi-Evaporator Vapor Compression Systems

Danielson, C.

TR2017-149 October 2017

Abstract

Multi-evaporator vapor compression systems (ME-VCS) are inherently multiinput multi-output (MIMO) systems, often with complex, highly coupled dynamics. Thus, they require more sophisticated control schemes than traditional on-off logic, or decentralized proportional-integral controllers. Unfortunately, many MIMO control design techniques are not well suited for this problem since they require complex numerical computations that do not scale gracefully for the high-dimensional dynamics of ME-VCS systems. This paper exploits the observed similarity of the room dynamics to reduce the computational complexity of designing controllers. We use a linear matrix inequality based controller synthesis technique that exploits symmetry for designing controllers for large-scale ME-VCS systems. This controller synthesis technique was applied to an MEVCS system with 50 rooms. Using traditional control design methods required 41 hours to synthesize a controller, while our technique designed an identical controller in less than 1 second.

ASME Dynamic Systems and Control Conference

This work may not be copied or reproduced in whole or in part for any commercial purpose. Permission to copy in whole or in part without payment of fee is granted for nonprofit educational and research purposes provided that all such whole or partial copies include the following: a notice that such copying is by permission of Mitsubishi Electric Research Laboratories, Inc.; an acknowledgment of the authors and individual contributions to the work; and all applicable portions of the copyright notice. Copying, reproduction, or republishing for any other purpose shall require a license with payment of fee to Mitsubishi Electric Research Laboratories, Inc. All rights reserved.

Symmetric Control Design for Multi-Evaporator Vapor Compression Systems

Claus Danielson

June 12, 2017

Abstract

Multi-evaporator vapor compression systems (ME-VCS) are inherently multi-input multi-output (MIMO) systems, often with complex, highly coupled dynamics. Thus, they require more sophisticated control schemes than traditional on-off logic, or decentralized proportional-integral controllers. Unfortunately, many MIMO control design techniques are not well suited for this problem since they require complex numerical computations that do not scale gracefully for the high-dimensional dynamics of ME-VCS systems. This paper exploits the observed similarity of the room dynamics to reduce the computational complexity of designing controllers. We use a linear matrix inequality based controller synthesis technique that exploits symmetry for designing controllers for large-scale ME-VCS systems. This controller synthesis technique was applied to an ME-VCS system with 50 rooms. Using traditional control design methods required 41 hours to synthesize a controller, while our technique designed an identical controller in less than 1 second.

0.1 Introduction

Vapor compression systems, such as heat pump, refrigeration, and air-conditioning systems, are widely used in commercial and residential applications. Multi-evaporator vapor compression systems (ME-VCS) are a sub-class of vapor compression systems where an outdoor unit processes refrigerant that is distributed to multiple indoor units to provide heating or cooling to different thermal zones. Multi-evaporator vapor compression systems (ME-VCS) are inherently multi-input multi-output (MIMO) systems, often with complex, highly coupled dynamics. Thus, ME-VCS systems require more sophisticated control schemes than traditional on-off logic, or decentralized proportional-integral controllers [1, 2]. Unfortunately, many MIMO control design techniques are not well suited for this problem since they require complex numerical computations that do not scale gracefully for the high-dimensional dynamics of ME-VCS systems. This is especially a problem for multi-evaporator vapor compression systems with a large number of indoor units. This paper develops a simplified control synthesis technique for ME-VCS systems that has constant computational cost regardless of the number of indoor units.

It has been widely observed that the rooms/indoor units of ME-VCS systems often have similar dynamics [3, 4, 5]. Using the mathematical formalism of symmetry we can rigorously quantify this similarity and exploit it in control design. Symmetries are transformations of a system's inputs, outputs, and states for which the system is invariant. Symmetry has been used extensively to simplify control design [6, 7, 8, 9, 10, 11, 12, 13, 14]. In [6] the authors developed a linear matrix inequality (LMI) based controller design methodology that exploits symmetry to reduce computational complexity. The control synthesis from [6] requires that the user knows the symmetry group of their system and how this symmetry can be used to select input and output channels that decompose the system. A symmetry group of a system can be identified using the method from [15] and these symmetries can be used to decompose the system using the method from [16]. The results of [6, 15, 16] are based on highly abstract mathematics which can overwhelm practitioners who are only interested in applying the results. This paper provides a concrete tutorial for applying symmetric control design to ME-VCS systems. In this paper, we explicitly report a symmetry group commonly found in ME-VCS systems and provide an easily verifiable condition for testing whether a particular system is symmetric. This paper explicitly reports the input and output channels that decompose the dynamics of ME-VCS systems. Finally, we apply the decomposed control design from [6] to the decompose ME-VCS. The end result is an intuitive, computationally simple technique for synthesizing controllers for ME-VCS systems with a large number of indoor units.

This paper is organized as follows. In Section 0.2 we describe the ME-VCS and its existing control design procedure. In Section 0.3 we formally define symmetry and describe a symmetry group for the ME-VCS. Furthermore, we show how these symmetries can be used to decompose the ME-VCS model into decoupled subsystems. The emphasis of this section is explaining the hidden

insights that can be gained by applying the abstract theory of symmetry to ME-VCS systems. In Section 0.4 we show how to use symmetry to simplify controller synthesis for ME-VCS systems. Finally in Section 0.5 we validate the analysis and synthesis results presented in this paper using an empirical ME-VCS model.

0.2 ME-VCS Control System

In this section we describe the multi-evaporator vapor compression system (ME-VCS) and its baseline controller.

Multi-Evaporator Vapor Compression System

The ME-VCS is comprised of a single outdoor unit and r indoor units as shown in Figure 1. In cooling mode, the compressor in the outdoor unit increases the pressure and temperature of the refrigerant which then flows through the outdoor unit heat exchanger where it loses heat and condenses. The refrigerant is then distributed to the indoor units where it flows through an expansion valve and heat exchanger allowing the refrigerant to absorb heat from the corresponding room, lowering the room temperature. Inner control loops regulate the amount and quality of refrigerant in each indoor unit to produce a desired cooling command. A more detailed description of the ME-VCS can be found in [5].

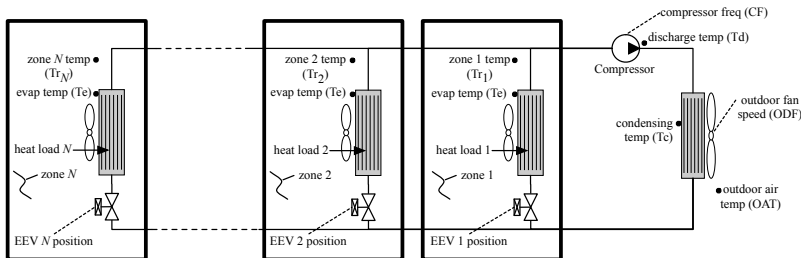


Figure 1: Schematic of the refrigerant flow in an r room ME-VCS system.

The inputs $u(t)$ of the ME-VCS are the compressor frequency CF, outdoor-fan speed ODF, and the cooling commands CC_i to each of the indoor units $i = 1, \dots, r$. The measured outputs $y(t)$ are the discharge T_d , discharge superheat T_{dsh} , condenser T_c , and evaporator T_e temperatures, and the room temperatures T_i for $i = 1, \dots, r$

The inputs are split into $r+1$ channels; the inputs for the outdoor unit $u_0(t) = [CF, ODF]^T$ and the inputs for the r indoor units $u_i(t) = CC_i$ for $i = 1, \dots, r$. Similarly, the outputs are split into $r+1$ channels; the outputs of the outdoor unit $y_0(t) = [T_d, T_{dsh}, T_c, T_e]^T$ and the outputs of the r indoor

units $y_i(t) = T_i$. The dynamics of the ME-VCS are model by the following linear discrete-time system

$$G = \left[\begin{array}{c|cccc} A & B_0 & B_1 & \cdots & B_r \\ \hline C_0 & D_{00} & D_{01} & \cdots & D_{0r} \\ C_1 & D_{10} & D_{11} & \cdots & D_{1r} \\ \vdots & \vdots & \vdots & \ddots & \vdots \\ C_r & D_{r0} & D_{r1} & \cdots & D_{rr} \end{array} \right]. \quad (1)$$

where $A \in \mathbb{R}^{n_x \times n_x}$, $B_i \in \mathbb{R}^{n_x \times n_u^i}$, $C_i \in \mathbb{R}^{n_y^i \times n_x}$, and $D_{ij} \in \mathbb{R}^{n_y^i \times n_u^j}$ for $i, j = 0, \dots, r$. We denote by G_{ij} the dynamics from the j -th input channel $u_j(t)$ for $j \in \{0, \dots, r\}$ to the i -th output channel $y_i(t)$ for $i \in \{0, \dots, r\}$ i.e.

$$G_{ij} = \left[\begin{array}{c|c} A & B_j \\ \hline C_i & D_{ij} \end{array} \right].$$

We make the following assumption about the system structure.

Assumption (Symmetry). *The ME-VCS satisfies:*

- *The dynamics G_{ii} relating the cooling capacity $u_i(t)$ to the room temperature $y_i(t)$ are the same for each indoor unit i.e. $G_{ii} = G_{jj}$ for all $i, j = 1, \dots, r$.*
- *The dynamics G_{ij} that model the coupling between indoor units are the same for every pair indoor units $G_{ij} = G_{kl}$ for all $i, j, k, l = 1, \dots, r$.*
- *The dynamics G_{i0} relating the compressor frequency and outdoor fan speed $u_0(t)$ to the i -th room temperature are the same for every room $G_{i0} = G_{j0}$ for all $i, j = 1, \dots, r$.*
- *The dynamics G_{0i} relating the i -th cooling capacity command $u_i(t)$ to the discharge, discharge super-heat, evaporator, and condenser temperatures $y_0(t)$ are the same for every indoor unit $G_{0i} = G_{0j}$ for all $i, j = 1, \dots, r$.*

The validity of Assumption 0.2 can be verified in a variety of ways e.g. analytically using the linear model (1), empirically through laboratory experiments, or semi-empirically through simulations of a more complex model.

Assumption 0.2 is an input-output property of the ME-VCS in the sense that it does not depend on how the ME-VCS was modeled, but rather a relationship between its inputs and outputs. This is an important distinction since the states of the linear model (1) do not necessarily have physical meaning and since the state-space realization (1) is not unique. Therefore, we cannot make assumptions about any structural properties of the state-space parameters (A, B, C, D). However, in this paper we will show that Assumption 0.2 can be used to reveal structure in the state-space matrices.

Control Objectives

The control objectives are to drive the room temperatures $y_i(t) = T_i$ to their desired reference set-points $T_{i,\text{rf}}$ with zero steady-state tracking error. Furthermore, the discharge temperature T_d should be driven to a reference set-point $T_{d,\text{rf}}$ chosen to improve energy efficiency. Thus, we define the reference signal

$y^\infty = [T_{d,\text{rf}}, T_{1,\text{rf}}, \dots, T_{r,\text{rf}}]^\top$ which includes the reference discharge temperature $T_{d,\text{rf}}$ and room temperatures $T_{i,\text{rf}}$ for $i = 1, \dots, r$. We assume that there exists at least one equilibrium state x^∞ and input u^∞ that produce the desired reference y^∞ .

In addition, the controller should limit unnecessary slewing of the control inputs. Thus, we will design an controller for the ME-VCS that penalizes the change $u(t) - u(t-1)$ in the control inputs between sample times.

Estimator and Controller Design

In this section we describe the current procedure for designing an estimator and controller for the ME-VCS. We highlight some of the computational issues with this procedure. In subsequent sections we will use symmetry to address these computational issues.

The ME-VCS uses a state-feedback controller where the state includes the actual plant state as well as the states of an input filter and output filter that capture the desired closed-loop behavior of the system. The control objectives specify that the room temperatures should be driven to the desired reference values and that the discharge temperature should be regulated to a set-point reference chosen to improve energy efficiency. These control objectives are captured by a filter W^{out} that acts on the plant outputs $y(t)$ and references y^∞ . The inputs of the performance filter W^{out} are the measured outputs $y(t)$ and the desired reference signals y^∞ of the ME-VCS. The states of the filter $\xi_i(t)$ integrate the room tracking errors $e_i(t) = y_i(t) - y_i^\infty$ for $i = 1, \dots, r$ so that the integral-action of the resulting controller will provide zero steady-state set-point tracking errors. The outputs $z(t) = [e_0(t), e_1(t), \dots, e_r(t), \xi_1(t), \dots, \xi_r(t)]^\top$ of the filter W^{out} include the discharge temperature tracking error e_0 , the room temperature tracking errors $e_i(t) = y_i(t) - y_i^\infty$, and the integrated room tracking errors $\xi_i(t)$. The output-filter is described by the following discrete-time linear system

$$W^{\text{out}} = \left[\begin{array}{c|cc} I_r & B_y^{\text{out}} & -B_{y^\infty}^{\text{out}} \\ \hline 0 & D_y^{\text{out}} & -D_{y^\infty}^{\text{out}} \\ 0 & B_y^{\text{out}} & -B_{y^\infty}^{\text{out}} \\ I_r & 0 & 0 \end{array} \right] \quad (2a)$$

where $B_y^{\text{out}} = [0, I]$ and $B_{y^\infty}^{\text{out}} = [0, I]$ extract the room temperatures $y_i(t)$ and the room temperature references y_i^∞ from the plant outputs $y(t)$ and references y^∞ respectively, and $D_y^{\text{out}} = [1, 0]$ and $D_{y^\infty}^{\text{out}} = [1, 0]$ extract the discharge temperature and discharge temperature reference from the measured outputs $y(t)$ and references y^∞ respectively. We denote by W_y^{out} and $W_{y^\infty}^{\text{out}}$ the response of the output-filter (2a) to measured outputs $y(t)$ and references y^∞ respectively.

The control objectives also specify that the controller should limit the slew rates of the control inputs. Thus, we use an input performance filter W^{in} that integrates the actuator slew rates to obtain the actual actuator commands. The inputs to the filter W^{in} are the incremental inputs $\delta u(t)$, the state $u(t-1)$ is the previous control input, and output is the current control input $u(t) =$

$u(t-1) + \delta u(t)$. The input-filter W^{in} is described by the following discrete-time linear system

$$W^{in} = \left[\begin{array}{c|c} I_{r+2} & I_{r+2} \\ \hline I_{r+2} & I_{r+2} \end{array} \right]. \quad (2b)$$

The ME-VCS model (1) and the performance filters (2) can be combined to form the augmented plant

$$W_y^{out} G W^{in} = \underbrace{\left[\begin{array}{ccc|c} I & B_y^{out} C & 0 & 0 \\ 0 & A & B & B \\ 0 & 0 & I & I \\ \hline 0 & D_y^{out} C & D_y^{out} D & D_y^{out} D \\ 0 & B_y^{out} C & D_y^{out} D & B_y^{out} D \\ I & 0 & 0 & 0 \end{array} \right]}_{\left[\begin{array}{c|c} \mathbf{A} & \mathbf{B} \\ \hline \mathbf{C} & \mathbf{D} \end{array} \right]}. \quad (3)$$

The ME-VCS uses a state-feedback controller that operates on the state $\mathbf{x}(t) = [\xi(t), x(t) - x^\infty, u(t-1) - u^\infty]^\top$ of the augmented system (3) to compute changes $\delta u(t) = u(t) - u(t-1)$ to the actuator commands $u(t)$ where the origin of the augmented state-space has been shifted to the desired equilibrium state x^∞ and input u^∞ . The feedback gain $\mathbf{F} = [F^\xi, F, F^u]$ is chosen to satisfy the Lyapunov equation

$$(\mathbf{A} + \mathbf{B}\mathbf{F})^\top \mathbf{P} (\mathbf{A} + \mathbf{B}\mathbf{F}) - \mathbf{P} \preceq -\mathbf{C}^\top \mathbf{Q} \mathbf{C} - \mathbf{F}^\top \mathbf{R} \mathbf{F} \quad (4)$$

where \mathbf{A} , \mathbf{B} , \mathbf{C} , and \mathbf{D} are the state-space matrices of the augmented system (3). The penalty matrices $\mathbf{R} \succ 0$ and $\mathbf{Q} \succ 0$ are design parameters used to reduce slewing of the control inputs or produce more aggressive set-point tracking respectively. The Lyapunov equation (4) guarantees that the controller achieves zero steady-state tracking error for set-point references.

The Lyapunov equation (4) used to design the feedback gain \mathbf{F} and Lyapunov matrix \mathbf{P} can be recast as a linear matrix inequality and solved using standard numerical tools [17]. However, solving these linear matrix inequalities can become intractable when the number of indoor units r is large i.e. $r \gg 1$. In Section 0.4, we will use the symmetry of the ME-VCS model (1) to decompose the Lyapunov equation (4) reducing the computational complexity of the control design.

The state $\mathbf{x}(t)$ of the augmented system (3) is estimated using a reduced-order observer. Since the states $\xi(t)$ and $u(t-1) - u^\infty$ of the filters (2) are measured directly, the observer only needs to estimate the shifted state $x(t) - x^\infty$ of the ME-VCS. The shifted state $x(t) - x^\infty$ is estimated using a Kalman filter where the observer gain $L = A \Sigma C^\top (V + C \Sigma C^\top)^{-1}$ is obtained by solving the standard discrete-time algebraic Riccati equation

$$\Sigma = A \Sigma A^\top + B W B^\top - A \Sigma C^\top (V + C \Sigma C^\top)^{-1} C \Sigma A^\top \quad (5)$$

where $V \in \mathbb{R}^{n_y \times n_y}$ is the covariance of the sensor noise and $W \in \mathbb{R}^{n_u \times n_u}$ is the covariance of the heat load disturbance.

The ME-VCS controller can then be described by the linear discrete-time

system

$$K = \left[\begin{array}{ccc|cc} I & 0 & 0 & B_y^{out} & B_{y^\infty}^{out} \\ BF^\xi & A+LC+BF & B(I+F^u) & -L & L \\ F^\xi & F & I+F^u & 0 & 0 \\ \hline F^\xi & F & I+F^u & 0 & G_{dc}^\dagger \end{array} \right] \quad (6)$$

where the controller inputs are the plant measurements $y(t)$ and the desired references y^∞ and the controller output $u(t)$ the actuator commands to the ME-VCS. The controller (6) has the same state $\mathbf{x}(t) = [\xi(t), x(t)-x^\infty, u(t-1)-u^\infty]^\top$ as the augmented system (3). The feedforward term $u^\infty = G_{dc}^\dagger y^\infty$ is an equilibrium input corresponding to the reference set-point y^∞ where G_{dc}^\dagger is a pseudo-inverse of the steady-state gain $G_{dc} = D+C(I-A)^{-1}B$ of the ME-VCS (1).

0.3 Decomposition of the ME-VCS using Symmetry

In this section we define symmetry and show how symmetry can be used to decompose a linear system. This decomposition is then used to decompose the ME-VCS model (1) and the performance filters (2). Since the symmetric decomposition is a direct consequence of Assumption 0.2, this decomposition is valid for any linear model (1) of the ME-VCS. This section uses theoretical results from [16] to analyze the structural properties of models of vapor-compression systems.

Definition of Symmetry

A symmetry of a dynamic system G is a pair of invertible transformations of the inputs $\Theta_u \in \mathbb{R}^{n_u \times n_u}$ and outputs $\Theta_y \in \mathbb{R}^{n_y \times n_y}$ that do not change the input-output behavior of the system

$$\Theta_y G = G \Theta_u \quad (7)$$

This definition says that the systems G and $\Theta_y^{-1}G\Theta_u$ have identical input-output behavior. Equivalently, definition (7) says that the response $y(t)$ of the systems G to the input $u(t)$ is related to the response $\Theta_y y(t)$ of the system to the input $\Theta_u u(t)$. We will index a set \mathfrak{G} of symmetries using the notation $\Theta_u(g)$ and $\Theta_y(g)$ for $g \in \mathfrak{G}$. Without loss of generality, we can assume that the set \mathfrak{G} is a group [18].

In practice, the precise definition of symmetry (7) is overly restrictive. Instead, we say a system G is approximately symmetric with respect to the group \mathfrak{G} if the condition (7) holds approximately

$$\|G - \Theta_y(g)^{-1}G\Theta_u(g)\|_\infty \leq \epsilon \quad (8)$$

for each element $g \in \mathfrak{G}$ of the group \mathfrak{G} where $\|\cdot\|_\infty$ is the \mathcal{H}_∞ -norm of a system. Definition (8) says that the systems G and $\Theta_y^{-1}G\Theta_u$ have approximately the same input-output behavior. In other words, the responses $y(t) = Gu(t)$ and $y'(t) = G'u(t)$ of the systems G and $G' = \Theta_y^{-1}G\Theta_u$ to the same input $u(t)$ are

approximately the same

$$\begin{aligned} \|y(t) - y'(t)\|_2 &= \|Gu(t) - \Theta_y^{-1}G\Theta_u u(t)\|_2 \\ &\leq \|G - \Theta_y^{-1}G\Theta_u\|_\infty \|u(t)\|_2 \leq \epsilon \|u(t)\|_2 \end{aligned}$$

where $\|\cdot\|_2$ is the \mathcal{L}_2 -norm of a signal. Note that the definition of approximate symmetry (8) is only applicable to stable systems, since the difference $y(t) - y'(t)$ between nearly identical but unbounded responses $y(t)$ and $y'(t)$ of the unstable systems G and $\Theta_y^{-1}G\Theta_u$ can be unbounded $\|y(t) - y'(t)\|_2 = \infty$.

Symmetries of the ME-VCS

In this section we define a group of symmetries for the ME-VCS model (1) and performance filters (2).

According to Assumption 0.2, the ME-VCS has symmetries of the form

$$\Theta_u = \begin{bmatrix} I_2 & 0 \\ 0 & \Theta \end{bmatrix}, \quad \Theta_y = \begin{bmatrix} I_4 & 0 \\ 0 & \Theta \end{bmatrix} \quad (9)$$

where $\Theta \in \mathfrak{S}_r \subset \mathbb{R}^{r \times r}$ is any permutation matrix. Thus, a symmetry group for the ME-VCS (1) is the (terribly named) symmetric group \mathfrak{S}_r [18].

The input symmetries Θ_u permute the cooling capacity commands $u_i(t)$ for each room $i = 1, \dots, r$ while leaving the compressor frequency and output fan speed $u_0(t)$ fixed. The output symmetries Θ_y permute the room temperature measurements $y_i(t)$ while leaving the discharge, discharge super-heat, evaporator, and compressor temperature $y_0(t)$ fixed. Thus, Assumption 0.2 is equivalent to saying that the definition of symmetry (7) holds for the symmetries (9). If the ME-VCS is open-loop stable, then we can use the definition of approximate symmetry (8) to relax Assumption 0.2, instead requiring that the equalities $G_{ij} = G_{lk}$ hold approximately $\|G_{ij} - G_{lk}\| \leq \epsilon$.

The performance filters (2) share a similar symmetric structure (9) as the ME-VCS. According to the definition of symmetry (7), the symmetries of the input performance filter (2b) are pairs of transformations $\Theta_u \in \mathbb{R}^{n_u \times n_u}$ and $\Theta_{\delta u} \in \mathbb{R}^{n_u \times n_u}$ that satisfy $\Theta_u W^{in} = W^{in} \Theta_{\delta u}$. In this case, the symmetries $\Theta_{\delta u}$ of the incremental inputs $\delta u(t)$ are the same $\Theta_{\delta u} = \Theta_u$ as the symmetries (9) of the inputs $u(t)$. These symmetries say that the input performance filter W^{in} applies the same filtering to each of the indoor unit inputs $u_i(t)$.

For the output performance filter (2a), we use a special case of the definition of symmetry (7) where the filter inputs $y(t)$ and y^∞ are transformed independently

$$\Theta_z W^{out} = W^{out} \begin{bmatrix} \Theta_y & 0 \\ 0 & \Theta_{y^\infty} \end{bmatrix}.$$

The transformation Θ_y of the ME-VCS outputs $y(t)$ was defined in (9). The transformations of the performance outputs $z(t)$ and references y^∞ are given by

$$\Theta_z = \begin{bmatrix} 1 & 0 & 0 \\ 0 & \Theta & 0 \\ 0 & 0 & \Theta \end{bmatrix}, \quad \Theta_{y^\infty} = \begin{bmatrix} 1 & 0 \\ 0 & \Theta \end{bmatrix} \quad (10)$$

where the permutation matrix $\Theta \in \mathfrak{S}_r \subset \mathbb{R}^{r \times r}$ is an element of the symmetric

group \mathfrak{S}_r . These symmetries (10) say the output performance filter W^{out} applies the same filtering to each of the room outputs $y_i(t)$ for $i = 1, \dots, r$.

The performance filters are only marginally stable. Thus, the definition of approximate symmetry (8) is not applicable since the \mathcal{H}_∞ -norm of the filters are unbounded. However, since these filters are purely mathematical (rather than modeling a physical phenomenon) we can ensure that their dynamics (2) satisfy the exact definition of symmetry (7).

Symmetric Decomposition

In this section we summarize how symmetry can be used to decompose a dynamic system into decoupled subsystems. The technical details can be found in [16].

The symmetric decomposition finds transformed input channels $\hat{u}_i(t) = \Phi_{u,i}^* u(t)$ that only affect the corresponding transformed output channel $\hat{y}_i(t) = \Phi_{y,i}^* y(t)$. The transformed input and output channels are defined by partitioned, orthogonal transformations of the form

$$\Phi_u = [\Phi_{u,1} \mid \dots \mid \Phi_{u,r}] \in \mathbb{R}^{n_u \times n_u} \quad (11a)$$

$$\Phi_y = [\Phi_{y,1} \mid \dots \mid \Phi_{y,r}] \in \mathbb{R}^{n_y \times n_y} \quad (11b)$$

where r is the number of input-output channel pairs and the sizes of the partitions $\Phi_{u,i} \in \mathbb{R}^{n_u \times \hat{n}_u^i}$ and $\Phi_{y,i} \in \mathbb{R}^{n_y \times \hat{n}_y^i}$ satisfy $\sum_{i=1}^r \hat{n}_u^i = n_u$ and $\sum_{i=1}^r \hat{n}_y^i = n_y$ respectively. Since the transformations (11) are orthogonal, the inverse transforms are given by $u(t) = \sum_{i=1}^r \Phi_{u,i} \hat{u}_i(t)$ and $y(t) = \sum_{i=1}^r \Phi_{y,i} \hat{y}_i(t)$ respectively. Throughout this paper, variables represented in the transformed domain (11) will be denoted with the hat $\hat{\cdot}$ notation.

Consider the subsystem $\hat{G}_{ij} = \Phi_{y,i}^* G \Phi_{u,j}$ that models the response of the i -th output channel $\hat{y}_i(t) = \Phi_{y,i}^* y(t)$ to the j -th input channel $\hat{u}_j(t) = \Phi_{u,j}^* u(t)$ given by

$$\hat{G}_{ij} = \left[\begin{array}{c|c} A & B\Phi_{u,j} \\ \hline \Phi_{y,i}^* C & \Phi_{y,i}^* D\Phi_{u,j} \end{array} \right]. \quad (12)$$

where (12) is not necessarily a minimal state-space realization of the system $\hat{G}_{ij} = \Phi_{y,i}^* G \Phi_{u,j}$. Using symmetry, the transformations (11) can be constructed such that the subsystem (12) between non-matching input $\hat{u}_j(t)$ and output $\hat{y}_i(t)$ channels $i \neq j$ has no observable and controllable dynamics. In other words, the minimal realization of the subsystem $\hat{G}_{ij} = 0$ is zero whenever $i \neq j$. Therefore, the transformations (11) decompose the system

$$\hat{G} = \Phi_y^* G \Phi_u = \begin{bmatrix} \hat{G}_{11} & & \\ & \ddots & \\ & & \hat{G}_{rr} \end{bmatrix} \quad (13)$$

Now consider the diagonal blocks $\hat{G}_{ii} = \Phi_{y,i}^* G \Phi_{u,i}$ corresponding to matching input and output channels $i = j$. Let \hat{n}_x^i be the number of states of a minimal realization of the system (12). Then we have $\sum_{i=1}^r \hat{n}_x^i = n_x$. Thus, the symmetric decomposition block diagonalizes (13) the system G while main-

taining the number of states. Furthermore, there exists a state-space transformation Φ_x that transforms the A matrix of the system G into the decomposed matrix $\hat{A} = \Phi_x^* A \Phi_x$ in (13). The i -th block $\Phi_{x,i}$ of the transformation $\Phi_x = [\Phi_{x,1}, \dots, \Phi_{x,r}]$ is the controllable and observable subspace of the Kalman decomposition of \hat{G}_{ii} [16]. Thus, we automatically obtain the state-space symmetric transformation Φ_x simply by computing minimal realizations of the subsystems \hat{G}_{ii} .

These results were extended to systems that are only approximately symmetric in [16]. For a stable, approximately symmetric (8) system G , the off-diagonal terms $\hat{G}_{ij} = \Phi_{y,i}^* G \Phi_{u,j}$ are small

$$\|\Phi_{y,i}^* G \Phi_{u,j}\|_\infty \leq \epsilon$$

where ϵ is the tolerance from the definition of approximate symmetry (8). Furthermore, each diagonal term $\Phi_{y,i}^* G \Phi_{u,i}$ is close to a stable system \hat{G}_{ii} with \hat{n}_x^i states i.e.

$$\|\hat{G}_{ii} - \Phi_{y,i}^* G \Phi_{u,i}\|_\infty \leq \epsilon.$$

Thus, we can approximate the system $\hat{G} = \Phi_y^* G \Phi_u$ by a decomposed system of the form (13) that preserves the number of states $\sum_{i=1}^r \hat{n}_x^i = n_x$ of the original system.

Decomposition of the ME-VCS

The symmetries (9) of the ME-VCS can be used to find symmetric transformations (11) that decompose (13) the dynamics (1) of the ME-VCS. The symmetric basis are given by

$$\Phi_u = \begin{bmatrix} I_2 & 0 \\ 0 & \Phi \end{bmatrix}, \quad \Phi_y = \begin{bmatrix} I_4 & 0 \\ 0 & \Phi \end{bmatrix} \quad (14)$$

where

$$\Phi = \left[\begin{array}{c|c|c|c} \frac{1}{r} & 1 & & \\ \frac{1}{r} & \frac{-1}{r-1} & & \\ \vdots & \vdots & \ddots & \\ \frac{1}{r} & \frac{-1}{r-1} & \dots & 1 \\ \hline & & & -1 \end{array} \right] \Lambda. \quad (15)$$

and Λ is a diagonal scaling matrix that normalizes the column vectors of Φ . The transformations (14) depend only on the symmetries (9) of the ME-VCS. Thus, we can use these transformations (14) to decompose any ME-VCS model (1) that satisfies Assumption 0.2. Details about numerical derivation of the transformations (14) can be found in [16].

Remark 1. *Scaling the transformations Φ_y and Φ_u via a diagonal matrices Λ_u and Λ_y will not change the decomposition (13) of the system $\hat{G} = \Lambda_y^{-1} \Phi_y^* G \Phi_u \Lambda_u$. Therefore, we will drop the matrix Λ from (15) when defining the input $\hat{u} = \Lambda_u^{-1} \Phi_u^* u$ and output $\hat{y} = \Lambda_y^{-1} \Phi_y^* y$ channels in order to make the results of this section more intuitive where $\Lambda_u = \begin{bmatrix} I_2 & 0 \\ 0 & \Lambda \end{bmatrix}$ and $\Lambda_y = \begin{bmatrix} I_4 & 0 \\ 0 & \Lambda \end{bmatrix}$. This diagonal scaling Λ can then be absorbed in the dynamics $\hat{G} = \Lambda_y^{-1} \Phi_y^* G \Phi_u \Lambda_u$. \square*

The partitioned transformations (14) split the inputs $u(t)$ and output $y(t)$ of the ME-VCS into r channels. The first output channel $\hat{y}_1(t) = \Lambda_{y,1}^{-1} \Phi_{y,1}^* y(t)$ is comprised of the outdoor unit outputs $y_0(t)$ and the average temperature $\frac{1}{r} \sum_{i=1}^r y_i(t)$ of all the rooms

$$\hat{y}_1(t) = \left[\begin{array}{c} y_0(t) \\ \frac{1}{r} \sum_{i=1}^r y_i(t) \end{array} \right]. \quad (16a)$$

For $i = 2, \dots, r$, the output channel $\hat{y}_i(t) = \Lambda_{y,i}^{-1} \Phi_{y,i}^* y(t)$ is the deviation of the $(i-1)$ -th room temperature $y_{i-1}(t)$ from the average of last $r-i+1$ room temperatures

$$\hat{y}_i(t) = y_{i-1}(t) - \frac{1}{r-i+1} \sum_{j=i}^r y_j(t). \quad (16b)$$

The inputs $u(t)$ of the ME-VCS are similarly split into r channels. The first input channel $\hat{u}_1(t) = \Lambda_{u,1}^{-1} \Phi_{u,1} u(t)$ is comprised of the outdoor unit inputs $u_0(t)$ and the average cooling command $\frac{1}{r} \sum_{i=1}^r u_i(t)$ for all the indoor units

$$\hat{u}_1(t) = \left[\begin{array}{c} u_0(t) \\ \frac{1}{r} \sum_{i=1}^r u_i(t) \end{array} \right]. \quad (17a)$$

For $i = 2, \dots, r$, the input channel $\hat{u}_i(t) = \Lambda_{u,i}^{-1} \Phi_{u,i} u(t)$ is the deviation of the $(i-1)$ -th cooling command $u_{i-1}(t)$ from average of the last $r-i+1$ cooling commands

$$\hat{u}_i(t) = u_{i-1}(t) - \frac{1}{r-i+1} \sum_{j=i}^r u_j(t). \quad (17b)$$

The subsystem $\hat{G}_{11} = \Lambda_{y,1}^{-1} \Phi_{y,1}^* G \Phi_{u,1} \Lambda_{u,1}$ that models the response of the first output channel (16a) to the first input channel (17a) has the form

$$\hat{G}_{11} = \begin{bmatrix} G_{00} & rG_{01} \\ G_{10} & G_{11} + (r-1)G_{12} \end{bmatrix} \quad (18a)$$

where G_{00} models the dynamics of outdoor unit, $G_{11} = G_{ii}$ models the internal dynamics of the indoor units, G_{01} and G_{10} model the coupling between the indoor and outdoor units, and $G_{12} = G_{ij}$ models the coupling between the indoor units. Intuitively, the subsystem (18a) models the ME-VCS as an outdoor unit connected to one large fictitious indoor unit that models the combined load of all r indoor units. The effect rG_{01} of the average cooling command $\frac{1}{r} \sum_{i=1}^r u_i(t)$ on the outdoor unit outputs $y_0(t)$ is r times larger than the effect G_{01} of a single cooling command $u_1(t)$. If there is no coupling between the indoor units $G_{12} = 0$, the dynamics from average cooling command $\frac{1}{r} \sum_{i=1}^r u_i(t)$ to average room temperature $\frac{1}{r} \sum_{i=1}^r y_i(t)$ are exactly the same as the dynamics G_{11} of a single room. When the indoor units are coupled $G_{12} \neq 0$, the coupling effect $(r-1)G_{12}$ becomes more apparent in the average room temperature $\frac{1}{r} \sum_{i=1}^r y_i(t)$ as the number r of indoor units increases.

The subsystems $\hat{G}_{ii} = \Lambda_{y,i}^{-1} \Phi_{y,i}^* G \Phi_{u,i} \Lambda_{u,i}$ that model the response of the i -th output channel (16b) to the i -th input channel (17b) are identical and have the form

$$\hat{G}_{ii} = G_{11} - G_{12} \quad (18b)$$

for $i = 2, \dots, r$. Intuitively, the decoupled subsystems (18b) model only the internal dynamics of the room with the coupling dynamics G_{12} between rooms

removed.

For $i \neq j$, the j -th input channel (17b) has no effect on the i -th output channel (16b) and thus the subsystem $\hat{G}_{ij} = \Phi_{y,i}^* G \Phi_{u,j} = 0$ has no observable and controllable dynamics. Therefore, the symmetric transformations (14) decomposes the ME-VCS model (1) into r decoupled subsystems.

The performance filters (2) can also be decomposed using symmetry. The output-filter (2a) is decomposed by a transformation Φ_z on its outputs $z(t)$ and a pair of transformations Φ_y and Φ_{y^∞} on its inputs $y(t)$ and y^∞ respectively. The transformation Φ_y is the same as the transformation (14) of the ME-VCS outputs $y(t)$. The transformations Φ_{y^∞} and Φ_z on the references y^∞ and performance outputs $z(t)$, respectively, are given by

$$\Phi_{y^\infty} = \begin{bmatrix} 1 & 0 \\ 0 & \Phi \end{bmatrix}, \quad \Phi_z = \begin{bmatrix} 1 & 0 & 0 \\ 0 & \Phi & 0 \\ 0 & 0 & \Phi \end{bmatrix} \quad (19)$$

where Φ was defined in (15). The transformation Φ_{y^∞} splits the references y^∞ into r channels. The first reference channel $\hat{y}_1^\infty(t)$ is comprised of the reference discharge temperature y_0^∞ and the average reference temperatures for each of the rooms

$$\hat{y}_1^\infty(t) = \begin{bmatrix} y_0^\infty(t) \\ \frac{1}{r} \sum_{i=1}^r y_i^\infty(t) \end{bmatrix}. \quad (20a)$$

For $i = 2, \dots, r$, the reference channel $\hat{y}_i^\infty(t)$ is the deviation of the $(i-1)$ -th reference temperature y_{i-1}^∞ from the average of the last $r-i+1$ reference temperatures

$$\hat{y}_i^\infty(t) = y_{i-1}^\infty(t) - \frac{1}{r-i+1} \sum_{j=i}^r y_j^\infty(t). \quad (20b)$$

The i -th transformed reference $\hat{y}_i^\infty(t) = \hat{y}_i^\infty$ corresponds to an equilibrium state $\hat{x}_i^\infty = \Phi_{x,i}^* x^\infty$.

The transformation Φ_z in (19) splits the performances outputs $z(t)$ into r channels. The first performance channel $\hat{z}_1(t)$ is comprised of the discharge temperature error $z_0(t)$, the average room temperature error, and the average integrated room temperature error

$$\hat{z}_1(t) = \begin{bmatrix} z_0(t) \\ \frac{1}{r} \sum_{i=1}^r e_i(t) \\ \frac{1}{r} \sum_{i=1}^r \xi_i(t) \end{bmatrix}. \quad (21a)$$

For $i = 2, \dots, r$, the performance channel $\hat{z}_i(t)$ is comprised of the deviation of temperature error $e_{i-1}(t)$ of the $(i-1)$ -th room from the average of the last $r-i+1$ temperature errors, and the deviation of integrated temperature error $\xi_{i-1}(t)$ of the $(i-1)$ -th room from the average of the last $r-i+1$ integrated errors

$$\hat{z}_i(t) = \begin{bmatrix} e_{i-1}(t) \\ \xi_{i-1}(t) \end{bmatrix} - \frac{1}{r-i+1} \sum_{j=i}^r \begin{bmatrix} e_j(t) \\ \xi_j(t) \end{bmatrix} \quad (21b)$$

for $i = 2, \dots, r$.

The following proposition characterizes the subsystems $\hat{W}_{y,ii}^{out} = \Phi_{z,i}^* W_y^{out} \Phi_{y,i}$ and $\hat{W}_{y^\infty,ii}^{out} = \Phi_{z,i} W_{y^\infty}^{out} \Phi_{y^\infty,i}$ that model the response of the i -th performance output channels (21) to the i -th measured output (16) and i -th reference (20)

channel.

Proposition 1. *The system \hat{W}^{out} has block-diagonal structure (13) with diagonal subsystems*

$$\hat{W}_{11}^{out} = \left[\begin{array}{c|cc} 1 & \hat{B}_y^{out} & -\hat{B}_{y^\infty}^{out} \\ 0 & \hat{D}_y^{out} & -\hat{D}_{y^\infty}^{out} \\ 0 & \hat{B}_y^{out} & -\hat{B}_{y^\infty}^{out} \\ 1 & 0 & 0 \end{array} \right] \quad \hat{W}_{ii}^{out} = \left[\begin{array}{c|cc} 1 & 1 & -1 \\ 0 & 1 & -1 \\ 1 & 0 & 0 \end{array} \right] \quad (22a)$$

for $i = 2, \dots, r$ where $\hat{B}_y^{out} = [\mathbf{0}, 1]$ and $\hat{B}_{y^\infty}^{out} = [0, 1]$ select the average room temperature and average room temperature reference from the output channel (16a) and reference channel (20a) respectively, and $\hat{D}_y^{out} = [1, \mathbf{0}]$ and $\hat{D}_{y^\infty}^{out} = [1, 0]$ select the discharge temperature and discharge temperature reference.

Proof. From the definitions (14) of Φ_y and (19) of Φ_z and Φ_{y^∞} , and the definition (2a) of W^{out} we have

$$\hat{W}_{ij}^{out} = \left[\begin{array}{c|cc} I & (0, \Phi_j) & (0, -\Phi_j) \\ 0 & (1, 0) & (1, 0) \\ 0 & (0, \Phi_i^* \Phi_j) & (0, -\Phi_i^* \Phi_j) \\ \Phi_i^* & 0 & 0 \end{array} \right].$$

The result (22a) follows from applying the state-space transformation $T = \Phi = [\Phi_1, \dots, \Phi_r]$ and removing the unobservable and uncontrollable states where $\Phi_i^* \Phi_i = I$ and $\Phi_i^* \Phi_j = 0$ for $i \neq j$. \square

The decomposed output filter (22a) operates on the transformed output (16) and reference (20) channels independently. This means that we can obtain the performance outputs $z(t)$ by independently filtering each output $\hat{y}_i(t)$ and reference $\hat{y}_i^\infty(t)$ channel and inverse-transforming the results $z(t) = \sum_{i=1}^r \Phi_{z,i} \hat{z}_i(t)$. Note that a similar decomposition is possible for any output-filter W^{out} that shares the symmetric structure (9) of the ME-VCS.

The input performance filter (2b) can be similarly decomposed. Since $\Theta_{\delta u} = \Theta_u$, the input-filter (2b) is decomposed by the input transformation Φ_u in (14) i.e. $\hat{W}^{in} = \Phi_u^* W^{in} \Phi_u$. The decomposed input filter has the form

$$\hat{W}_{11}^{in} = \left[\begin{array}{c|c} I_3 & I_3 \\ \hline I_3 & I_3 \end{array} \right] \quad \hat{W}_{ii}^{in} = \left[\begin{array}{c|c} 1 & 1 \\ \hline 1 & 1 \end{array} \right] \quad (22b)$$

for $i = 2, \dots, r$. The derivation of the input sub-filters (22b) is similar to the derivation of the output sub-filters (22a).

In the next section, we will exploit the decomposed structure of the ME-VCS model (18) and performance filters (22) to reduced the complexity of both control design and implementation.

0.4 Symmetric Control for the ME-VCS

In this section we show how symmetry can be used to reduce the computational complexity of designing controllers for the ME-VCS. Our control design methodology was inspired by [6].

Symmetric Estimator and Control Design

Our symmetric control design relies on the following simple fact.

Theorem. *A controller \hat{K} stabilizes the transformed system $\hat{G} = \Phi_y^* G \Phi_u$ if and only if the inverse-transformed controller $K = \Phi_u \hat{K} \Phi_y^*$ stabilizes the original system G .*

Proof. Closing the loop around the system $\Phi_y^* G \Phi_u \hat{K}$ is exactly the same as closing the loop around the system $G \Phi_u \hat{K} \Phi_y^*$. \square

This theorem means that we can design a stabilizing controller K for a system G by designing a controller \hat{K} for the transformed system $\hat{G} = \Phi_y^* G \Phi_u$. For a symmetric system (7), the transformed system \hat{G} is decomposed. Thus, we can design the controller \hat{K} by independently designing sub-controllers \hat{K}_{ii} that stabilize the decoupled subsystems \hat{G}_{ii} of \hat{G} .

For the ME-VCS, we need to design a controller for the aggregate subsystem (18a) and a controller \hat{K}_{22} for the deviation subsystem (18b). The controller for the aggregate subsystem (18a) will have the structure

$$\begin{bmatrix} \hat{K}_{00} & \hat{K}_{01} \\ \hat{K}_{10} & \hat{K}_{11} \end{bmatrix}$$

where \hat{K}_{00} is the sub-controller for the outdoor unit, \hat{K}_{11} is the sub-controller for the average indoor unit dynamics, and \hat{K}_{01} and \hat{K}_{10} are the sub-controllers for the coupling between the outdoor unit and average indoor unit. The deviation subsystem controller \hat{K}_{22} can then be repeated $r-1$ times to obtain a controller \hat{K} for an ME-VCS with r indoor units. The controllers \hat{K} in the transformed domain can then be inverse-transformed to obtain a controller K for the ME-VCS (1) in the original domain

$$\begin{aligned} K &= \Phi_u \hat{K} \Phi_y^* = \\ &= \begin{bmatrix} \hat{K}_{00} & 0 & \cdots & 0 \\ \hat{K}_{10} & \hat{K}_{22} & & \\ \vdots & & \ddots & \\ \hat{K}_{10} & & & \hat{K}_{22} \end{bmatrix} + \frac{1}{r} \begin{bmatrix} 0 & \hat{K}_{01} & \cdots & \hat{K}_{01} \\ 0 & \hat{K}_{11} - \hat{K}_{22} & \cdots & \hat{K}_{11} - \hat{K}_{22} \\ \vdots & \vdots & \ddots & \vdots \\ 0 & \hat{K}_{11} - \hat{K}_{22} & \cdots & \hat{K}_{11} - \hat{K}_{22} \end{bmatrix}. \end{aligned} \quad (23)$$

Thus, we can build a controller for the ME-VCS with an arbitrary number r of indoor units by designing two small controllers for the aggregate subsystem (18a) and the deviation subsystem (18b). In practice, the dimension of the models of the outdoor unit G_{00} , a single indoor unit G_{11} and their interactions G_{01} , G_{01} , and G_{12} do not depend on the total number of indoor units r . Thus, the dimension of the two ME-VCS subsystems (18) is typically constant. Therefore, the computational complexity of synthesizing the symmetric controller (23) remains constant, regardless of the number r of indoor units.

The design of the decoupled controllers \hat{K} for the ME-VCS subsystems (18) follows a procedure analogous to the design of the baseline controller (6). The

controllers for the ME-VCS subsystems (18) have the form

$$\hat{K}_{ii} = \left[\begin{array}{ccc|cc} I & 0 & 0 & \hat{B}_{y,i}^{out} & \hat{B}_{y^\infty,i}^{out} \\ \hat{B}_i \hat{F}_i^\xi & \hat{A}_i + \hat{L}_i \hat{C}_i + \hat{B}_i \hat{F}_i & \hat{B}_i (I + \hat{F}_i^u) & -L_i & L_i \\ \hat{F}_i^\xi & \hat{F}_i & I + \hat{F}_i^u & 0 & 0 \\ \hline \hat{F}_i^\xi & \hat{F}_i & I + \hat{F}_i^u & 0 & \hat{G}_i^\top \end{array} \right] \quad (24)$$

for $i = 1, 2$ where the state $\hat{\boldsymbol{x}}_i(t) = [\hat{\xi}_i(t), \hat{x}_i(t) - \hat{x}_i^\infty, \hat{u}_i(t-1) - \hat{u}_i^\infty]^\top$ of the i -th controller is comprised of the state $\hat{\xi}_i(t)$ of the i -th output filter (22a), the estimated shifted state $\hat{x}_i(t) - \hat{x}_i^\infty$ of the i -th ME-VCS subsystem (18), and the shifted state $\hat{u}_i(t-1) - \hat{u}_i^\infty$ of the i -th input filter (22b).

The feedback gain $\hat{\boldsymbol{F}}_i = [\hat{F}_i^\xi, \hat{F}_i, \hat{F}_i^u]$ is chosen to satisfy the decomposed Lyapunov equation

$$(\hat{\boldsymbol{A}}_{ii} + \hat{\boldsymbol{B}}_i \hat{\boldsymbol{F}}_i)^\top \hat{\boldsymbol{P}}_i (\hat{\boldsymbol{A}}_{ii} + \hat{\boldsymbol{B}}_i \hat{\boldsymbol{F}}_i) - \hat{\boldsymbol{P}}_i \preceq -\hat{\boldsymbol{C}}_i \hat{\boldsymbol{Q}}_i \hat{\boldsymbol{C}}_i - \hat{\boldsymbol{F}}_i^\top \hat{\boldsymbol{R}}_i \hat{\boldsymbol{F}}_i \quad (25)$$

where the weighting matrices $\hat{\boldsymbol{Q}}_{ii} \succ 0$ and $\hat{\boldsymbol{R}}_{ii} \succ 0$ penalize the performance outputs $\hat{z}_i(t)$ and incremental inputs $\delta \hat{u}_i(t)$ for the i -th ME-VCS subsystem (18) respectively. The matrices $\hat{\boldsymbol{A}}_i$, $\hat{\boldsymbol{B}}_i$, $\hat{\boldsymbol{C}}_i$, and $\hat{\boldsymbol{D}}_i$ are the state-space matrices of a minimal realization of the augmented subsystem

$$\hat{W}_{y,ii}^{out} \hat{G}_{ii} \hat{W}_{ii}^{in} = \underbrace{\left[\begin{array}{ccc|c} I & \hat{B}_{y,ii}^{out} \hat{C}_{ii} & 0 & 0 \\ 0 & \hat{A}_{ii} & \hat{B}_{ii} & \hat{B}_{ii} \\ 0 & 0 & I & I \\ \hline 0 & \hat{D}_{y,ii}^{out} \hat{C}_{ii} & \hat{D}_{y,ii}^{out} \hat{D}_{ii} & \hat{D}_{y,ii}^{out} \hat{D}_{ii} \\ 0 & \hat{B}_{y,ii}^{out} \hat{C}_{ii} & \hat{D}_{y,ii}^{out} \hat{D}_{ii} & \hat{B}_{y,ii}^{out} \hat{D}_{ii} \\ I & 0 & 0 & 0 \end{array} \right]}_{\left[\begin{array}{c|c} \hat{\boldsymbol{A}}_i & \hat{\boldsymbol{B}}_i \\ \hline \hat{\boldsymbol{C}}_i & \hat{\boldsymbol{D}}_i \end{array} \right]} \quad (26)$$

for $i = 1, 2$. The state of the augmented subsystem (26) is estimated using a reduced-order observer where only the offset state $\hat{x}_i(t) - \hat{x}_i^\infty$ of the ME-VCS subsystem (18) is estimated. The observer gain $\hat{L}_i = \hat{A}_i \hat{\Sigma}_i \hat{C}_i (\hat{V}_i + \hat{C}_i \hat{\Sigma}_i \hat{C}_i^\top)^{-1}$ for the i -th controller (24) is obtained by solving the discrete-time algebraic Riccati equation (5) with the state-space matrices from the i -th ME-VCS subsystem (18) and noise covariance matrices \hat{V}_i and \hat{W}_i .

Symmetric Estimator and Control Analysis

In this section we examine the conditions under which the symmetrically designed controller (23) is identical to the baseline controller (6). We begin by inverse-transforming the symmetric feedback $\hat{\boldsymbol{F}}_i$ and observer \hat{L}_i gains into the original domain. The inverse-transformation of the feedback gains $\hat{\boldsymbol{F}}_i$ and Lyapunov matrices $\hat{\boldsymbol{P}}_i$ is given by

$$\boldsymbol{F} = \sum_{i=1}^r \Phi_{u,i}^* \hat{\boldsymbol{F}}_i \Phi_{x,i} \quad (27a)$$

$$\boldsymbol{P} = \sum_{i=1}^r \Phi_{x,i}^* \hat{\boldsymbol{P}}_i \Phi_{x,i} \quad (27b)$$

where $\Phi_{x,i}^* = [\Phi_{y,i}^*, \Phi_{x,i}^*, \Phi_{u,i}^*]$ is the state-space transformations that maps the state $[\xi(t), x(t), u(t-1)]$ of the augmented system (3) to the state $[\hat{\xi}(t), \hat{x}(t), \hat{u}(t-1)]$ of the transformed augmented system (26).

Similarly, the observer gains \hat{L}_i and estimation error covariance matrices $\hat{\Sigma}_i$ can be inverse-VCS transformed to obtain an observer gain L and covariance matrix Σ for the ME-VCS (1) in the original domain

$$L = \sum_{i=1}^r \Phi_{x,i}^* \hat{L}_i \Phi_{y,i} \quad (28a)$$

$$\Sigma = \sum_{i=1}^r \Phi_{x,i}^* \hat{\Sigma}_i \Phi_{x,i} \quad (28b)$$

where Φ_x is the state-space transformation that such that $\Phi_x A \Phi_x^{-1} = \hat{A}$.

The following proposition shows that the observer gain and covariance matrix (28) are the identical to the baseline designs if temperature sensors and heat loads for each room have the same second-order statistics.

Proposition 2. *Let the covariance matrices $V = \Theta_y^* V \Theta_y$ and $W = \Theta_u^* W \Theta_u$ be symmetric. Then the observer gain and covariance matrix (28) are identical to those produced by the baseline design procedure in Section 0.2.*

Proof. Let \hat{L} and $\hat{\Sigma} \succ 0$ be the block-diagonalization of the matrices \hat{L}_{ii} and $\hat{\Sigma}_{ii}$ respectively. Then $\hat{\Sigma}$ satisfies the Riccati equation

$$\hat{\Sigma} = \hat{A} \hat{\Sigma} \hat{A}^\top + \hat{B} \hat{W} \hat{B}^\top - \hat{A} \hat{\Sigma} \hat{C}^\top (\hat{V} + \hat{C} \hat{\Sigma} \hat{C}^\top)^{-1} \hat{C} \hat{\Sigma} \hat{A}^\top$$

where $\hat{W} = \Phi_x^* W \Phi_x$ and $\hat{V} = \Phi_y^* V \Phi_y$ are block-diagonal since $V = \Theta_y^* V \Theta_y$ and $W = \Theta_u^* W \Theta_u$. Pre-multiplying by Φ_x^* and post-multiplying by Φ_x shows that covariance matrix $\Sigma = \Phi_x^* \hat{\Sigma} \Phi_x \succ 0$ is the unique positive definite solution of the Riccati equation (5) in the original domain since $\Phi_x^* \hat{A} \Phi_x = A$, $\Phi_x^* \hat{B} \Phi_u = B$, and $\Phi_y \hat{C} \Phi_x^* = C$ and $\Phi_x \Phi_x^* = I$, $\Phi_u \Phi_u^* = I$, and $\Phi_y \Phi_y^* = I$. Furthermore, the observer gain (28a) is identical to the original

$$\begin{aligned} L &= \Phi_x^* \hat{L} \Phi_y = \Phi_x^* \hat{A} \hat{\Sigma} \hat{C}^\top (\hat{V} + \hat{C} \hat{\Sigma} \hat{C}^\top)^{-1} \Phi_y \\ &= A \Sigma C^\top (V + C \Sigma C^\top)^{-1} \end{aligned}$$

since $\Phi_x^* \hat{A} \Phi_x = A$ and $\Phi_y \hat{C} \Phi_x^* = C$, and $\Phi_x \Phi_x^* = I$ and $\Phi_y \Phi_y^* = I$. \square \square

A similar results does not necessarily hold for the feedback gain and Lyapunov matrix (27) even when the weighting matrices $Q = \Theta_z^* Q \Theta_z$ and $R = \Theta_u^* R \Theta_u$ place the same penalty on the tracking errors and integrated tracking errors for each room temperature. This is because the Lyapunov equation (4) can have multiple solutions, some of which may be non-symmetric. However, if the inequalities in the original (4) and decomposed (25) Lyapunov equations are replaced with equality (i.e. they become Riccati equations), then the feedback gain and Lyapunov matrix (27) are identical to those obtained using the baseline approach. Similarly, if the Lyapunov equations are combined with a cost function that is convex and symmetric, then the feedback gain and Lyapunov matrix (27) will be identical to the baseline design [6]. In either of these cases, it can be shown that the baseline (6) and symmetric (23) controllers are identical.

0.5 Modeling and Design Validation

In this section we validate the analysis and design results presented in this paper.

Validation of the Model Decomposition

In this section we demonstrate the validity of model decomposition presented in Section 0.3.

The symmetric transformations (9) were applied to an empirically identified model of a $r = 2$ indoor unit ME-VCS. Figure 2 shows the frequency-dependent maximum singular values of the transformed subsystems $\hat{G}_{ij} = \Phi_{y,i}^* G \Phi_{u,j}$ for $i, j = 1, 2$. According to the theoretical results presented in Section 0.3 the off-diagonal subsystems \hat{G}_{12} and \hat{G}_{21} should be exactly zero. Since the empirically identified ME-VCS model G is only approximately symmetric, these subsystems \hat{G}_{12} and \hat{G}_{21} are non-zero as shown in Figure 2(b) and Figure 2(c). However, these subsystems \hat{G}_{12} and \hat{G}_{21} are stable and nearly zero $O(\|\hat{G}_{12}\|_\infty) = 10^{-16}$ and $O(\|\hat{G}_{21}\|_\infty) = 10^{-17}$. In contrast, the frequency responses of the diagonal subsystems \hat{G}_{11} and \hat{G}_{22} are 16 orders of magnitude larger $O(\|\hat{G}_{11}\|_\infty) = 1$ and $O(\|\hat{G}_{22}\|_\infty) = 1$. Thus, we expect the asymmetry of the ME-VCS dynamics to have negligible effect on the control design.

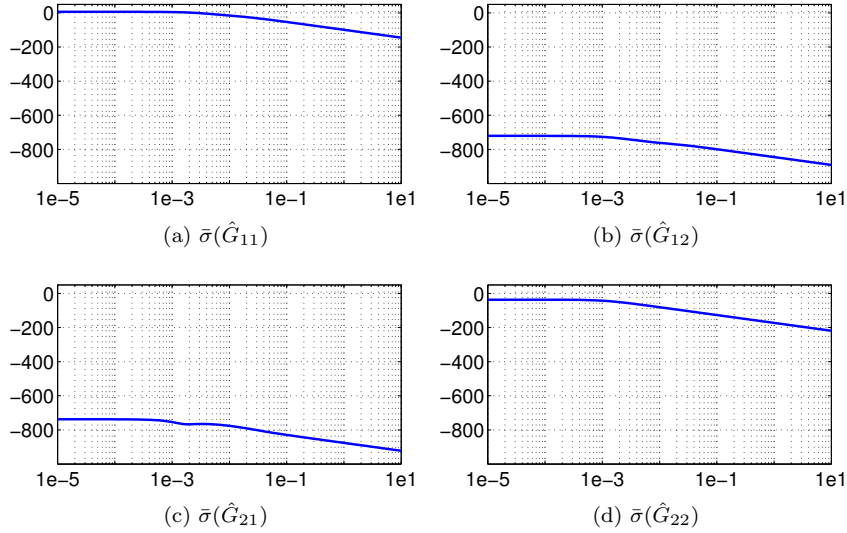


Figure 2: Bode magnitude plots for the decomposed ME-VCS subsystems (18).

Validation of the Control Design

In this section we demonstrate the validity of decomposed control design methodology presented in Section 0.4.

We designed a controllers for the $r = 2$ indoor unit ME-VCS from the previous section using the baseline procedure (6) and the symmetry exploiting procedure (23). For the baseline controller (6) the observer gain L_{base} was

obtained by solving the Riccati equation (5) and the feedback gain \mathbf{F}_{base} was obtained by solving the Lyapunov equation (4) with equality. For the symmetric controller (23) the observer gain L_{sym} was assembled (28a) from the sub-gains \hat{L}_{ii} obtained by solving the Riccati equation (5) for each of the ME-VCS subsystems (18). The feedback gain \mathbf{F}_{sym} was assembled (27a) from the sub-gains $\hat{\mathbf{F}}_{ii}$ obtained by solving the decomposed Lyapunov equation (25) with equality. The difference between the feedback and observer gains obtained using these two different procedures is minuscule $O(\|L_{base} - L_{sym}\|_F) = 10^{-14}$ and $O(\|\mathbf{F}_{base} - \mathbf{F}_{sym}\|_F) = 10^{-8}$ where $\|\cdot\|_F$ is the Frobenius-norm of a matrix.

Figure 3 shows the bode magnitude plots of the discharge and room temperature tracking errors in response to the changes in the discharge and room temperature references for both the baseline (6) and symmetric (23) controllers. Figure 3 shows that the closed-loop behavior $CL(G, K_{base})$ and $CL(G, K_{sym})$ produced by the baseline and symmetric controller are nearly identical $O(\|CL(G, K_{base}) - CL(G, K_{sym})\|_\infty) = 10^{-7}$.

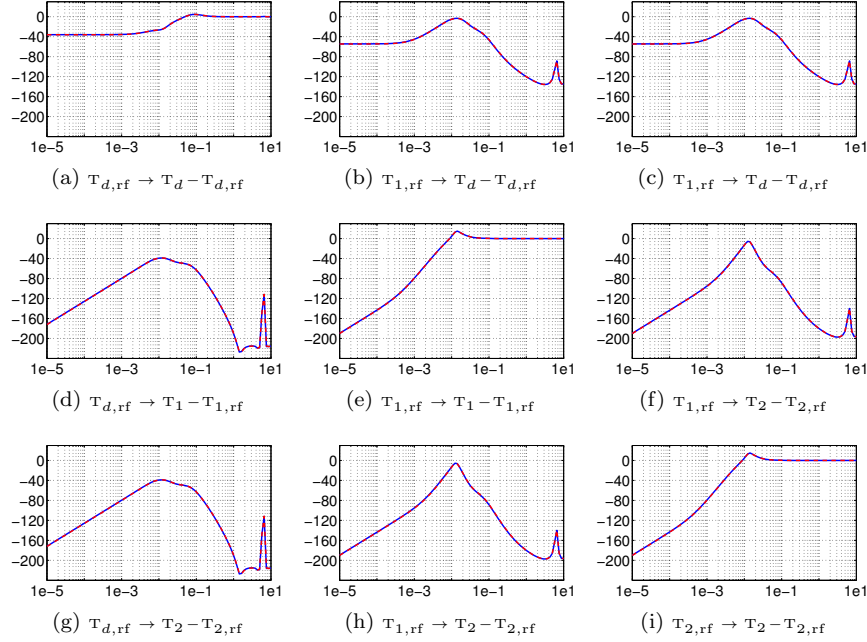


Figure 3: Closed-loop response of the discharge temperature T_d and room temperatures T_1 and T_2 tracking errors to changes in the references $T_{d,rf}$, $T_{1,rf}$, and $T_{2,rf}$. Solid blue-line is the baseline closed-loop response and dashed red-line is the symmetric closed-loop response.

Since the baseline (6) and symmetric (23) controllers produce identical closed-loop behavior, either can be used to design a controller for the ME-VCS. The

advantage of the symmetric control design is that the number and size of the Riccati equations or linear matrix inequalities that need to be solved to obtain the feedback \mathbf{F} and observer L gains is constant regardless of the number of indoor units r . On the other hand, the baseline procedure becomes increasingly complex as the number of indoor units r increase. We used the baseline and symmetric control design procedures to design a controller for an ME-VCS with $r = 50$ indoor units. The resulting baseline augmented plant (3) is very large, having 52 inputs, 101 outputs, 155 states, and 51 references. On the other hand, the decomposed augmented subsystems (26) are much smaller. The aggregate augmented subsystem (26) has 3 inputs, 3 outputs, 8 states, and 2 references. The $r - 1 = 49$ augmented deviation subsystems (26) each have 1 input, 2 outputs, 3 states and 1 reference. Furthermore, we only need to design a single controller \hat{K}_{22} for each of these $r - 1 = 49$ identical subsystems. Thus, the symmetric design procedure is significantly faster than the baseline procedure. The symmetry design procedure required less than 1 second, while the baseline design procedure required 41 hours to compute an identical controller.

0.6 Conclusions

This paper presented a controller synthesis procedure for ME-VCS systems. This procedure exploits the symmetry often observed in ME-VCS systems to reduce the computational complexity of designing controllers. To facilitate this control design procedure, we described a group of symmetries commonly found in ME-VCS systems and showed how these symmetries can be used to decompose an ME-VCS model and the performance filter used in the control design. This method was applied to a 50 unit ME-VCS resulting in a significant reduction in computation time.

Acknowledgements

The author would like to thank Georgios Stathopoulos, Stefano Di Cairano, and Dan Burns for their contributions in improving this paper.

Bibliography

- [1] He, X., Liu, S., Asada, H., and Itoh, H., 1998. “Multivariable control of vapor compression systems”. *HVAC&R Research*.
- [2] Koeln, J. P., and Alleyne, A. G., 2013. “Decentralized Controller Analysis and Design for Multi-Evaporator Vapor Compression Systems”. In American Control Conference.
- [3] Koehler, S., and Borrelli, F., 2013. “Building temperature distributed control via explicit mpc and trim and respond methods”. In European Control Conference.
- [4] Koeln, J., and Alleyne, A., 2014. “Scalable model predictive control for multi-evaporator vapor compression systems”. In American Control Conference.
- [5] Burns, D., Danielson, C., Zhou, J., and Di Cairano, S., 2016. “Reconfigurable model predictive control for multi-evaporator vapor compression systems”. *Transactions of Control Systems Technology*.
- [6] Cogill, R., Lall, S., and Parrilo, P., 2008. “Structured semidefinite programs for the control of symmetric systems”. *Automatica*, May.
- [7] Danielson, C., and Borrelli, F., 2012. “Symmetric explicit model predictive control”. In Nonlinear Model Predictive Control Conference.
- [8] Danielson, C., 2014. “Symmetric constrained optimal control: Theory, algorithms, and applications”. PhD thesis, University of California, Berkeley.
- [9] Chuang, F., Danielson, C., and Borrelli, F., 2014. “Optimality of certainty equivalence in expected value problems for uncertain linear systems optimality of certainty equivalence in expected value problems for uncertain linear systems”. In Conference on Decision and Control.
- [10] Danielson, C., and Borrelli, F., 2015. “Symmetric linear model predictive control”. *Transactions on Automatic Control*, May.
- [11] Danielson, C., and Di Cairano, S., 2015. “Reduced complexity control design for symmetric LPV systems”. In Conference on Decision and Control.

- [12] Chuang, F., Danielson, C., and Borrelli, F., 2015. “Robust approximate symmetric model predictive control”. In Conference on Decision and Control.
- [13] Danielson, C., and Borrelli, F., 2015. “Symmetric constrained optimal control”. In Nonlinear Model Predictive Control Conference.
- [14] Rufino Ferreira, A., Meissen, C., Arcak, M., and Packard, A., 2017. “Symmetry reduction for performance certification of interconnected systems”. *Transactions on Control of Network Systems*.
- [15] Danielson, C., and Borrelli, F., 2014. “Identification of the symmetries of linear systems with polytopic constraints”. In American Control Conference.
- [16] Danielson, C., and Bauer, S., 2015. “Numerical decomposition of symmetric linear systems”. In Conference on Decision and Control.
- [17] Boyd, S., El Ghaoui, L., Feron, E., and Balakrishnan, V., 1994. *Linear matrix inequalities in system and control theory*. SIAM.
- [18] Lang, S., 2002. *Algebra*. Springer.